


Cite this: *RSC Sustainability*, 2024, 2, 2581

## Eco-friendly amidation of oxidized carbon black by dry ball milling†

Aida Kiani, Marco Palumbo and Maria Rosaria Acocella \*

An unprecedented amidation of oxidized carbon black (oCB) by a mechanochemical approach is reported. The reaction proceeds in the presence of octadecylamine (ODA) in a short time, providing the corresponding adduct (oCB/ODA) with a high degree of functionalization. Hummers and ball milling procedures were used to obtain oxidized carbon black in solution and solvent-free conditions, respectively. Although the oxidation procedure used for oCB synthesis can deeply affect the degree of amidation because of the different nature of the functional groups on the carbon surface, the resulting powders were both functionalized with amine. The corresponding adducts showed a strong inversion of polarity, going from the high dispersibility in the water solution of the starting material to the high hydrophobic behaviour due to the alkyl chains bonded on the surface. Since the mechanochemical approach respects important green metrics, the procedure is highly sustainable.

Received 3rd May 2024  
Accepted 18th July 2024

DOI: 10.1039/d4su00216d

rsc.li/rscsus

### Sustainability spotlight

Carbon materials are widely used in many applications such as catalysts, energy storage and conversion, supercapacitors, and water remediation and mainly in polymer composites because of their exceptional influence on polymer properties. Specifically, carbon black is extensively used as a cost-effective and readily available carbon material whose physical properties can be deeply modified by introducing new functional groups, which makes it versatile for all possible purposes. Although the introduction of new functional groups as well as different molecules bonded onto the carbon surface is a well-known strategy, all the syntheses reported until now have been performed in organic solvents and under very harsh conditions, failing to meet environmental sustainability expectations. In this context, we envisioned the development of our procedure that, by using a mechanochemical approach, is able to provide covalent functionalization on the carbon surface for generating new materials for hydrophobic coating. By using a long chain alkylamine, octadecylamine (ODA), the ball milling action was shown to be effective at achieving a highly functionalized adduct under solvent-free conditions. Typical adducts display a strong inversion of polarity, with the starting material being highly dispersible in water and the adducts showing high hydrophobic behavior. By respecting important green metrics, we demonstrate new perspectives for developing new materials using a mechanochemical approach that appears to be a safe strategy for honoring sustainability requirements.

## Introduction

Carbon materials such as graphite, graphene, carbon nanotubes, and carbon black are widely used in many applications such as catalysts,<sup>1–5</sup> energy storage<sup>6–8</sup> and conversion,<sup>9,10</sup> supercapacitors,<sup>11</sup> and water remediation<sup>12</sup> and mainly in composites of polymers because of their exceptional influence on polymer properties.<sup>13–19</sup> The ability to improve the physical and mechanical properties of polymer matrices has made these materials attractive and the subject of many research studies.

Among them, carbon black (CB) is extensively used because it is waste from the incomplete combustion of petroleum derivatives and is cheap and readily available. Additionally, interest in this material has grown due to the ease of

introducing new functional groups on the surface, which makes it versatile for all possible purposes.

To chemically modify the carbon surface, it is essential to introduce oxygen functional groups to make a further step of modification possible.

Carbon black has been functionalized by introducing oxygen-containing groups through several methods, *e.g.*, Staudenmaier,<sup>20</sup> Hofmann,<sup>21,22</sup> Hummers,<sup>23</sup> and sulfonitric treatment.<sup>24</sup> However, most of them require expensive and toxic reagents and very harsh conditions to obtain a high oxidation degree, which fails to meet environmental sustainability expectations.

A high degree of oxidation has recently been achieved by using planetary ball milling under solvent-free conditions at room temperature with carbon black,<sup>25</sup> pointing out the new perspectives for carbon materials to be chemically modified using the mechanochemical approach.

Based on green parameters (*e.g.*, the E-factor, the EcoScale, energy demand, and CO<sub>2</sub> production), this procedure is more

Dipartimento di Chimica e Biologia and INSTM Research Unit, Università degli Studi di Salerno, Via Giovanni Paolo II 132, Fisciano, 84084, Italy. E-mail: macocella@unisa.it

† Electronic supplementary information (ESI) available. See DOI: <https://doi.org/10.1039/d4su00216d>



environmentally friendly than previous H<sub>2</sub>O<sub>2</sub> (ref. 26 and 27) or ozone oxidation<sup>28,29</sup> methods.

As recently reported,<sup>30</sup> further manipulations of oxidized carbon black (oCB) can be achieved using the mechanochemical approach by starting from oCB in the presence of a phosphonium salt. This sustainable functionalization is able to generate a new filler with flame retardant and/or antimicrobial properties.

The mechanochemical functionalization provides the adduct *via* cation exchange under solvent-free conditions in a short time, exploiting the acidic functionalities present on the surface.

Accordingly, the energy that comes from the collision of the balls during milling can facilitate the formation of covalent bonds, as well as ion exchange, allowing oxygen and cations to be introduced.

The choice of milling parameters, such as the speeding rate, ball-to-powder ratio, reaction time, and the nature of the balls, can profoundly affect the success of both procedures.

The need to functionalize the carbon surface derives from the possibility of deeply modifying the physical properties depending on the application required.

The introduction of long alkyl chains by using alkylamines, for instance, can increase the hydrophobic character of the carbon material, making it completely water-repellent.<sup>31,32</sup>

This modification can be obtained through the amidation reaction of oxidized carbon materials, *i.e.*, graphite oxide, oxidized nanotubes, and oxidized carbon black, characterized by the presence of carboxyl groups on the surface and the amine residue of the chosen alkylamine. The reaction usually takes place in an organic solvent using coupling agents<sup>33,34</sup> or under solvent-free conditions in a glass reactor, increasing the temperature to 180 °C and using high amine loading to promote amide conversion.<sup>35</sup>

This work aims to show the effectiveness of the ball milling action on carbon materials to obtain covalent functionalization on the surface by using amine.

As a matter of fact, many reports of covalent bond formation are disclosed for organic molecule synthesis<sup>36,37</sup> induced by mechanochemical action, but, to the best of our knowledge, no examples are reported for the covalent amine functionalization of carbon black by ball milling.

## Materials and methods

Carbon black samples (CB) of grade N110, containing 99.8% carbon and with BET surface area 130 m<sup>2</sup> g<sup>-1</sup>, were purchased from Cabot Company (USA). Sulfuric acid, sodium nitrate, potassium permanganate, and octadecyl amine (ODA) were purchased from Sigma-Aldrich. All reagents were used as received, without purification.

### Oxidation of carbon black *via* Hummers' method

Oxidized carbon black (oCB) was prepared using Hummers' method. 12 mL of sulfuric acid and 0.25 g of sodium nitrate were introduced into a 1000 mL three-neck round-bottomed

Table 1 Experimental conditions of the ball milling experiments

Ball-to-powder weight ratio	150
Rotation frequency [min <sup>-1</sup> ]	500
Ball size [mm]	10
Total balls weight [g]	15
Milling tool material	Silicon nitride
Beaker volume [cm <sup>3</sup> ]	80
CB weight [mg]	100
Sample notation	oCB <sub>BM</sub>

flask immersed in an ice bath and 0.5 g of carbon sample was added, with magnetic stirring. Once uniform dispersion was achieved, 1.5 g of potassium permanganate was added very slowly to minimize the risk of explosion. The reaction mixture was then heated to 35 °C and stirred for 24 hours. Afterward, 70 mL of deionized water was gradually added to the resulting black and dark green slurry, followed by the gradual addition of 0.5 mL of hydrogen peroxide 30 wt%; the obtained sample was poured into 700 mL of deionized water and then centrifuged at 10 000 rpm for 15 min with a Neya16 centrifuge. The oCB powder was first washed twice with 10 mL of a 5 wt% HCl aqueous solution and subsequently washed with 50 mL of deionized water. Finally, the powder was dried at 60 °C for 12 h. About 0.4 g of the oCB sample was obtained.

### Preparation of oCB *via* ball milling

The ball-milling experiments were conducted at room temperature on a planetary ball mill Pulverisette 7 Premium (Fritsch GmbH, Germany).

The milling conditions were configured as detailed in Table 1. Each procedure utilized 8 silicon nitride balls with a diameter of 10 mm within an 80 mL silicon nitride jar. Rotational frequencies were fixed at 500 rpm for 11 h. An Easy-GTM system (Fritsch GmbH, Germany) was used to measure the temperature of the milling beakers.

### Preparation of oCB<sub>H</sub>/ODA and oCB<sub>BM</sub>/ODA *via* ball milling

The experiment was performed in an 80 mL silicon nitride jar with 8 silicon nitride balls and 300 rpm rotational frequencies by using a 1/1 mass ratio of oCB<sub>H</sub> or oCB<sub>BM</sub> and ODA for 2 h. The resulting powders were extensively washed only with ethanol (90 mL) to remove the excess amine, and the amine was recovered for reuse after evaporation of ethanol. The products were dried at 60 °C for 12 h in an oven and were recovered as black powders.

To investigate the imine formation, the second part of the prepared oCB<sub>BM</sub>/ODA was washed extensively first with water and then with ethanol (90 mL) to remove the possible free amine coming from the ketone deprotection. The resulting powder was dried at 60 °C for 12 h in the oven.

## Results and discussion

Oxidized carbon black (oCB) samples derived from the Hummers oxidation (oCB<sub>H</sub>) and ball milling oxidation (oCB<sub>BM</sub>)



were chosen as reference materials to evaluate the best method of oxidation to proceed before amidation. The different natures of the functional groups present on the carbon surface can deeply affect the amidation reaction to provide the best performance.

Therefore, first, the characterization of  $\text{oCB}_\text{H}$  and  $\text{oCB}_\text{BM}$  was performed using FTIR, XRD, BET, and elemental analysis.

The FTIR evidences some important differences concerning the nature of the carbonyl group present on the surface (Fig. 1A). Specifically, while the region between 1300 and 1000  $\text{cm}^{-1}$  is quite similar, with a comparable distribution of ethers, vinyl ethers, and alcohols for both oxidation procedures, the nature of the carbonyl group is deeply affected. In particular, the Hummers oxidation promotes the formation of carboxyl acid with characteristic vibration at 1715  $\text{cm}^{-1}$ , while the ball milling oxidation promotes the possible formation of unsaturated ketones and lactones<sup>25</sup> with typical vibration at 1700  $\text{cm}^{-1}$ .

Therefore, the fragmentation and exfoliation during the milling drive the carbon material to react with the air oxygen and provide new oxygen functional groups whose nature can be different from that of the oxidation in solution. As a result, changing the oxidation procedure makes it possible to control the functional groups on the carbon surface.

The different degrees of oxidation were evaluated by elemental analysis, which showed a slightly higher O/C ratio of 0.44 for the  $\text{oCB}$  obtained by Hummer's oxidation (Table 2), as confirmed by the TGA analysis (Fig. 2A).

The increasing disorder induced by the milling action on the already amorphous carbon is evidenced by the X-ray diffraction pattern (Fig. 1B). The amorphous halo centered about at  $2\theta = 24^\circ$  is broadened because of the milling treatment that also provides  $\text{oCB}_\text{BM}$  with a higher surface area (291  $\text{m}^2 \text{g}^{-1}$ ) than  $\text{oCB}_\text{H}$  (125  $\text{m}^2 \text{g}^{-1}$ ).

Based on recent reports about the possibility of performing amidation by the mechanochemical approach under solvent-free conditions with small molecules,<sup>36,37</sup> we decided to

Table 2 Elemental analysis of the  $\text{oCB}$  samples

Entry	Sample	N (%)	C (%)	H (%)	O (%)	O/C	H/C	N/C
1	$\text{oCB}_\text{H}$	0.3	68	1.5	30.2	0.44	0.02	0.004
2	$\text{oCB}_\text{BM}$	1.1	71	0.5	27	0.38	0.007	0.015
3	$\text{oCB}_\text{H}/\text{ODA}$	3.0	79.7	6.3	11.0	0.14	0.08	0.04
4	$\text{oCB}_\text{BM}/\text{ODA}$	2.8	89	5.6	2.6	0.029	0.06	0.031
5	$\text{oCB}_\text{BM}/\text{ODA}^a$	2.3	76.0	5.0	16.7	0.22	0.07	0.030

<sup>a</sup> The sample was washed with water and then with ethanol.

evaluate the ability first of  $\text{oCB}_\text{H}$  and then of  $\text{oCB}_\text{BM}$  to react with octadecyl amine (ODA) in planetary milling and under solvent-free conditions.

The experiment was performed in an 80 mL silicon nitride jar with 8 silicon nitride balls at a 300 rpm speeding rate by using a 1/1 mass ratio of the  $\text{oCB}_\text{H}$  or  $\text{oCB}_\text{BM}$  and ODA.

After 2 h of milling and extensive washing with ethanol to remove the excess amine, the product was recovered as a black powder and characterized by FTIR, TGA, XRD, and elemental analysis.

As reported in Fig. 1A, interesting changes were found for the  $\text{oCB}_\text{H}/\text{ODA}$  adduct. The FTIR spectrum of  $\text{oCB}_\text{H}/\text{ODA}$  evidences the vibrations at 2953, 2917, 2846, and 717  $\text{cm}^{-1}$  related to the  $-\text{CH}_2$  stretching of the octadecyl chain and N-H wagging, respectively. Moreover, a sensible decrease of the carbonyl stretching at 1715  $\text{cm}^{-1}$ , the appearance of a shoulder at 1526  $\text{cm}^{-1}$ , possibly due to the C-N amide stretching,<sup>38</sup> and the blue shift from 1475  $\text{cm}^{-1}$  in the free amine to 1462  $\text{cm}^{-1}$  in the  $\text{oCB}_\text{H}/\text{ODA}$ , confirm the occurrence of the amidation. It is worth noting that the presence of epoxide on oxidized carbon cannot exclude possible amine functionalization by epoxy ring opening.

Additional characterization was performed on the resulting powder to reveal the possible free amine after the reaction. As shown in Fig. 1B, the X-ray diffraction pattern of the product does not evidence any crystalline peak due to the free amine, confirming the complete removal of excess ODA.

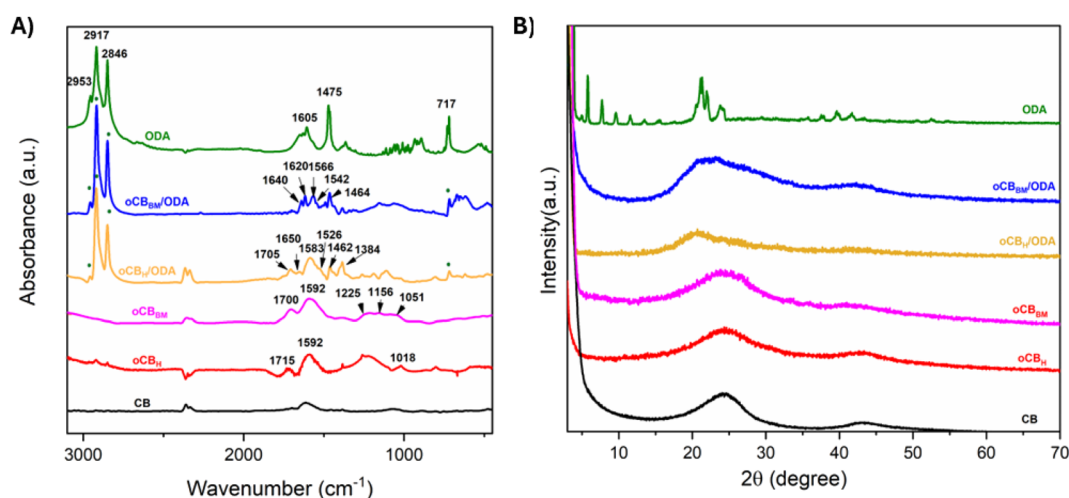


Fig. 1 FTIR (A) and X-ray diffraction patterns (B) of CB (black),  $\text{oCB}_\text{H}$  (red),  $\text{oCB}_\text{BM}$  (pink),  $\text{oCB}_\text{H}/\text{ODA}$  (yellow),  $\text{oCB}_\text{BM}/\text{ODA}$  (blue), and ODA (green).



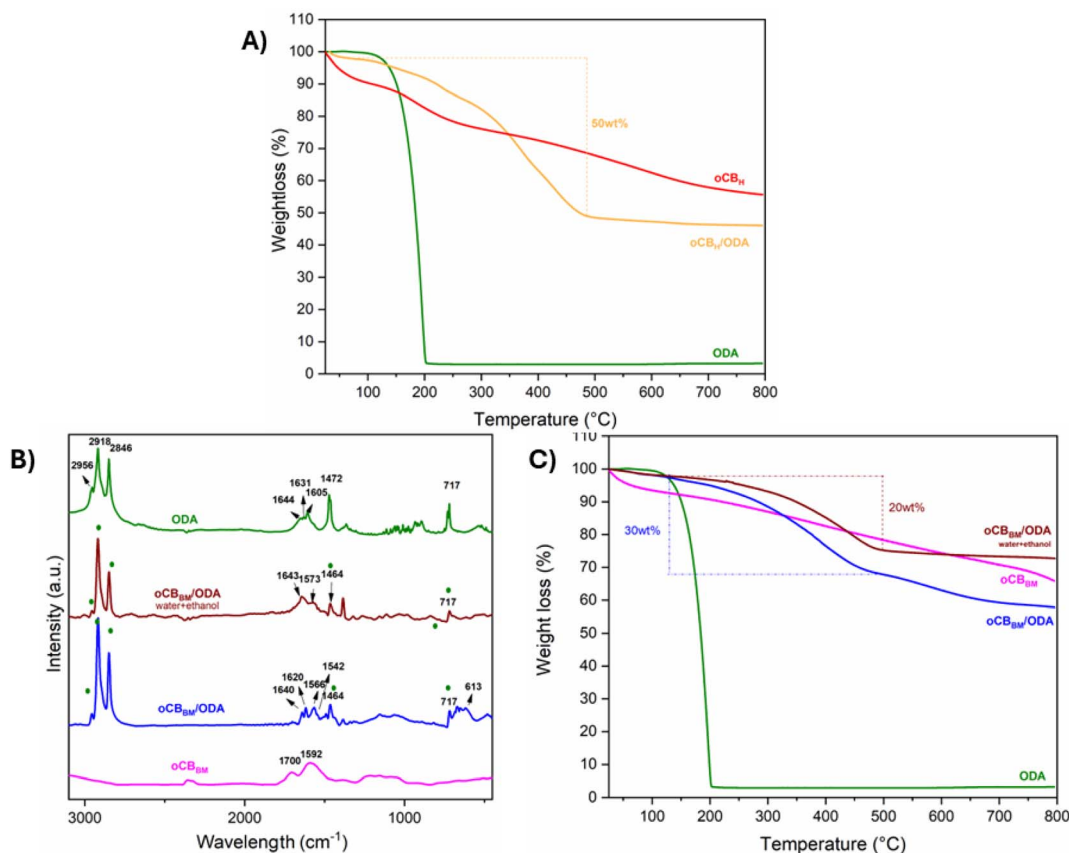
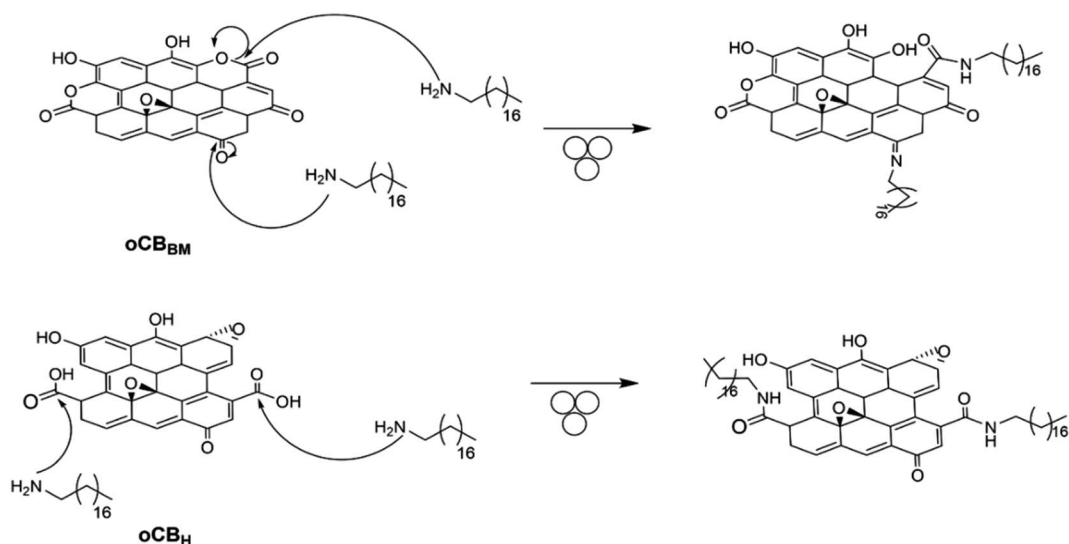


Fig. 2 (A) TGA of oCB<sub>H</sub> (red), ODA (green), and oCB<sub>H</sub>/ODA (yellow); (B) FTIR and (C) TGA of oCB<sub>BM</sub>/ODA before (blue) and after washing (wine) with water and ethanol in comparison with oCB<sub>BM</sub> (pink) and ODA (green).

As reported in a precedent paper<sup>39</sup> alkyl amines can provide hydrogen bonds of neutral or protonated amines, as well as ionically bound protonated amines on the oxidized graphitic surface. Therefore, additional washing steps under acidic conditions (pH = 4.5 and then 2) were performed on the derived

oCB<sub>H</sub>/ODA adduct. FTIR and EA confirmed no variation in the peak's intensity and the elemental composition, respectively (see the ESI<sup>†</sup>).

More surprisingly, interesting results were also obtained starting from oCB<sub>BM</sub>. Although ball milling oxidation does not



Scheme 1 Mechanism of functionalization of oCB<sub>BM</sub> and oCB<sub>H</sub> with ODA.



provide carboxyl groups on the carbon surface, it does provide ketones and lactones, which are useful functional groups that react with amines. Specifically, while lactones are suitable for the amidation reaction, ketones are instead able to provide imines (Scheme 1).

The different nature of the functional groups on  $\text{oCB}_{\text{BM}}$  is also evident from FTIR after the reaction. As reported in Fig. 1A, a more complex pattern is recorded for  $\text{oCB}_{\text{BM}}/\text{ODA}$ . Specifically, the  $1700\text{ cm}^{-1}$  band related to the carbonyl groups disappears and a vibration band at  $1620\text{ cm}^{-1}$  comes to light possibly due to imine formation,<sup>40</sup> as well as a vibration at  $1640\text{ cm}^{-1}$  and a shoulder at  $1542\text{ cm}^{-1}$  related to the amide. Again, the vibrations at 2953, 2917, 2846, and  $717\text{ cm}^{-1}$  related to the  $-\text{CH}_2$  stretching of the octadecyl chain and N-H wagging, respectively, and the blue shift from 1475 to  $1464\text{ cm}^{-1}$  are clearly observed also for  $\text{oCB}_{\text{BM}}/\text{ODA}$ .

The X-ray diffraction pattern of the adduct also shows a broadened halo centered at  $2\theta = 22^\circ$  due to the additional milling treatment, and no crystalline peaks are observed, confirming that there is no excess of free amine.

More interesting information was derived from the elemental analysis (Table 2). Comparing the nitrogen content of the starting materials,  $\text{oCB}_{\text{H}}$  and  $\text{oCB}_{\text{BM}}$ , with the resulting adducts, a higher uptake of nitrogen is recorded for  $\text{oCB}_{\text{H}}/\text{ODA}$  (entry 3 vs. 1, Table 2) than  $\text{oCB}_{\text{BM}}/\text{ODA}$  (entry 4 vs. 2, Table 2). The slightly higher oxidation degree, as well as the content of carboxyl groups, implicate higher functionalization through the amidation reaction.

Furthermore, the oxygen content is strongly reduced from 27% of the starting  $\text{oCB}_{\text{BM}}$  to 2.6% in  $\text{oCB}_{\text{BM}}/\text{ODA}$ , possibly due to the formation of imines.

Being an equilibrium reaction with water as a side product, the reaction can be driven into complete imine formation, exploiting the ability of the carbonaceous material to act as a scavenger of water.<sup>41</sup> Conversely, in the presence of water, the equilibrium is shifted to the reagent with the formation of ketones again.

Based on the typical mechanism of imine formation (Scheme 2), it becomes evident that in the presence of water, the imine should be removed, and only the amide provided by the mechanochemical reaction with lactones should still be present in  $\text{oCB}_{\text{BM}}/\text{ODA}$ .

Therefore,  $\text{oCB}_{\text{BM}}/\text{ODA}$  was extensively washed with water and then with ethanol to remove the possible free amine coming from the ketone deprotection. After drying at  $60^\circ\text{C}$ , the resulting powder was analyzed by FTIR, EA, and TGA.

As shown in Fig. 2B, a dramatic change in the FTIR spectra is detected after the water treatment. In particular, the vibration at  $1643$  and  $1541\text{ cm}^{-1}$  related to carbonyl and C-N stretching of amide, respectively, are evident, as are the bands at 2953, 2917, 2846, and  $717\text{ cm}^{-1}$  typical of the starting amine, while  $1620\text{ cm}^{-1}$  stretching related to the imine disappears. Additionally a broad band in the  $1680\text{--}1700\text{ cm}^{-1}$  region appears to be possibly related to the ketone deprotection.

The elemental analysis agrees with the FTIR results, showing a reduction of the nitrogen content and an enhanced percentage of oxygen due to the deprotection of ketone functionalities (entry 5, Table 2).

In addition, thermogravimetric analysis confirms that all the samples considered display different levels of functionalization. As reported in Fig. 2A,  $\text{oCB}_{\text{H}}/\text{ODA}$  shows a 50% weight loss, much higher than the 30% observed for  $\text{oCB}_{\text{BM}}/\text{ODA}$  (Fig. 2B). After water treatment, the  $\text{oCB}_{\text{BM}}/\text{ODA}$  adduct shows a further reduction in weight loss to 20 wt% due to the removal of imine. It has to be noted that in all cases, the weight losses are in good agreement with the amount of nitrogen detected by the EA (see the ESI†).

### Dispersibility tests

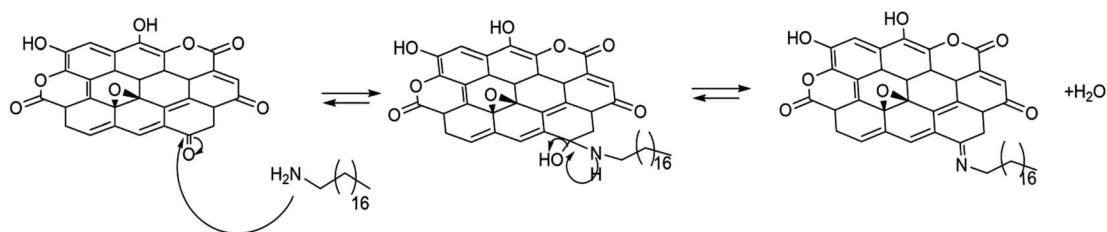
As previously reported,<sup>31,32</sup> amine functionalization deeply changes the polarity of  $\text{oCB}$ , making it strongly hydrophobic because of the presence of long alkyl chains.

To evaluate the polarity changes, dispersibility tests were conducted in the presence of water, ethyl acetate, and toluene chosen as reference solvents based on their polarity parameters<sup>42</sup> of 10, 4.4, and 2.3, respectively.

The surface modification by the amidation reaction caused a profound variation in the polarity of the  $\text{oCB}$  powders (Fig. 3).

This is particularly evident when comparing the solubility in water of both the powders,  $\text{oCB}_{\text{H}}$  and  $\text{oCB}_{\text{BM}}$ , with the corresponding  $\text{oCB}/\text{ODA}$  adducts. Specifically, very hydrophobic materials were provided by the mechanochemical functionalization of  $\text{oCB}_{\text{H}}$  and  $\text{oCB}_{\text{BM}}$  that strongly repel water and are stratified on the surface, generating a hydrophobic coating. The behaviour is different in ethyl acetate:  $\text{oCB}_{\text{H}}/\text{ODA}$  still results in a dispersible sediment in the solvent due to its residual polar functional groups (*i.e.*, alcohols, ethers, *etc.*), while  $\text{oCB}_{\text{BM}}/\text{ODA}$  precipitates as a non-dispersible sediment due to the conversion of ketones and lactones of the starting  $\text{oCB}_{\text{BM}}$  into imines and amides with the corresponding reduction of oxygen content (2.6%, see Table 2 entry 4).

As expected, both the  $\text{oCB}/\text{ODA}$  adducts are well dispersed in toluene as an apolar solvent.



Scheme 2 Mechanism of imine formation of  $\text{oCB}_{\text{BM}}$  with ODA.



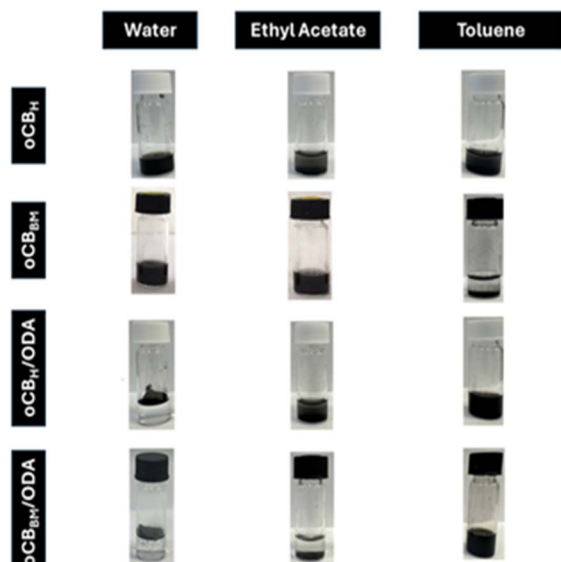


Fig. 3  $\text{oCB}_\text{H}$ ,  $\text{oCB}_\text{BM}$ ,  $\text{oCB}_\text{H}/\text{ODA}$ , and  $\text{oCB}_\text{BM}/\text{ODA}$  suspension in water, ethyl acetate, and toluene solution  $5 \text{ mg mL}^{-1}$  after 5 min of sonication and 30 min of storage.

### Sustainability evaluation of the process: green metrics

To show the effectiveness and greener character of the mechanochemical approach, a direct comparison with the less impactful procedure reported until now for the amidation of the carbon material, *i.e.*, graphite oxide, under solvent-free conditions<sup>33</sup> is proposed here.

As a matter of fact, while the reaction by using a coupling agent in DMF or thionyl chloride and DMF under heating is clearly not sustainable, the amidation procedure under solvent-free conditions seems to be relatively eco-friendly. Taking into account the condition to operate under vacuum, the total heating time, and the high weight ratio between the oxidized carbon material and ODA, 1 to 5, respectively, reported in ref. 33, the evaluation of the green parameters was performed considering the atom efficiency (AE), the reagent mass efficiency (RME), the process mass intensity (PMI), the EcoScale, energy demand, and  $\text{CO}_2$  production associated with the process (greenhouse gas equivalents).

Atom economy is a measure of the conversion efficiency of a chemical process, which is extremely useful for predicting how much waste the process will generate. Conversely, RME takes yields and the molar quantities of reactants into account, evidencing the reagent excess used in the reaction. It is

a realistic metric to illustrate how far from 'green' we are currently operating our processes. PMI is defined as "the total mass of materials used to produce a specified mass of product".<sup>43</sup> Therefore, a value close to 1 means that all the reagents are converted into the product, optimizing resource utilization. The E-factor is, instead, the effective amount of waste created.

In contrast, the EcoScale is a semiquantitative tool for selecting organic preparations that assigns penalty points based on a maximum value of 100 considering yield, cost, safety, and purification conditions.<sup>44</sup> This tool is particularly useful when the procedure moves from the laboratory to the industrial scale.

As part of the assessment, the energy required for each process needs to be included since energy consumption generates primarily waste, such as carbon dioxide.

The comparison between the amidation by heating and the mechanochemical process starting from  $\text{oCB}_\text{H}$  and  $\text{oCB}_\text{BM}$  is reported in Table 3 (for all the calculations, see the ESI†).

Based on the Heidolph data sheet, the energy required for keeping the reaction at  $180^\circ\text{C}$  for 3 h was calculated using  $0.800 \text{ kW}$ , as well as the ball mill's  $1.2 \text{ kW h}^{-1}$  energy consumption. It is worth noting that, although the energy demand, the  $\text{CO}_2$  production, and AE are similar, the solvent-free reaction induced by heating shows an RME lower than both the milling procedures due to the excess of the amine reagent with respect to the carbon material used (5 to 1 by weight).

As a result, the PMI value was closer to one for both  $\text{oCB}_\text{H}$  and  $\text{oCB}_\text{BM}$  reactions with amine by ball milling procedures and the corresponding E factors were lower than those for the heating/under vacuum treatment, providing a more eco-friendly procedure with a higher EcoScale value.

Therefore, even assuming a higher efficiency for the literature procedure, the RME, PMI, *E*, and EcoScale values make the ball milling procedure more environmentally sustainable.

To get a comprehensive evaluation of the green metrics, not only the waste generated during the process but also the one provided by the reagent synthesis should also be evaluated.

Hence, although the green metrics for the  $\text{oCB}_\text{H}$  amidation seem to be better than those of the corresponding reaction with  $\text{oCB}_\text{BM}$ , the oxidation process for  $\text{oCB}_\text{H}$  is based on the Hummers oxidation, characterized by toxic solvents and very harsh conditions. Therefore it is easy to understand that  $\text{oCB}_\text{BM}$ , which is an oxidized material obtained from a highly sustainable milling process, achieves the best eco-friendly performances for providing functionalized carbon materials.

Table 3 Comparison between the amidation by heating and ball milling procedures based on green metrics

Procedure	AE (%)	RME (%)	PMI	<i>E</i>	EcoScale <sup>a</sup> (%)	Energy demand (kW)	$\text{CO}_2$ production <sup>b</sup> (kg)
Heating, solvent-free	97	46	2.16	1.16	91.5	2.4	1
Ball milling $\text{oCB}_\text{H}$	97	65	1.54	0.5	95.5	2.4	1
Ball milling $\text{oCB}_\text{BM}$	94	57.5	1.7	0.7	95.5	2.4	1

<sup>a</sup> The EcoScale was evaluated based on the classification reported in ref. 43. <sup>b</sup> The  $\text{CO}_2$  production was evaluated based on the energy demand in  $\text{kW h}^{-1}$  for each process and converted into  $\text{CO}_2$  following the conversion factor reported by EPA (2020) AVERT, US Environmental Protection Agency, Washington, DC.



## Conclusions

The mechanochemical functionalization of oCB in the presence of octadecyl amine (ODA) under solvent-free conditions has been reported to proceed efficiently.

The study was performed, first comparing different oxidation methods for the carbon material, Hummers, and ball milling procedures to evidence the effect of the different nature of the functional groups in the amidation reaction step.

Although the oxidation procedures used for oCB synthesis can affect the degree of amidation because of the different nature of the functional groups present on the carbon surface, the resulting powders were both functionalized with amine. Specifically, the presence of carboxyl groups on the oCB by Hummers oxidation promotes amide formation with a degree of functionalization of 50 wt%, while the ketones and lactones of the oCB by milling oxidation provide imines and amides, respectively, with a degree of functionalization of 30 wt%.

Irrespective of the different functionalization degrees, the corresponding adducts showed both an inversion of polarity as long alkyl chains were introduced, which increased hydrophobicity and provided new fillers for water-repellent coatings.

Finally, to show the effectiveness and greener character of the mechanochemical approach, a direct comparison with the less impactful procedure reported until now for the amidation of carbon materials under solvent-free conditions was performed, also evaluating the impact of the synthetic procedure for the starting oCB.

Since the Hummers oxidation process for oCB involves toxic solvents and very harsh conditions, it is evident that the mechanochemical approach from the oCB synthesis to the amidation reaction achieves the best sustainability performance.

## Data availability

The data supporting this article have been included as part of the ESI.† The data that support the findings of this study are available from the corresponding author, M. R. A., upon reasonable request.

## Author contributions

M. R. A. contributed to the conception and design of the study, A. K. performed the experimental analysis and characterization, M. P. performed part of the experimental analysis, and M. R. A. and A. K. wrote the first draft of the manuscript. All authors contributed to the manuscript revision and read and approved the submitted version.

## Conflicts of interest

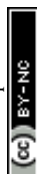
There are no conflicts to declare.

## Acknowledgements

Financial support of Ministero dell'Università e della Ricerca (MUR) is acknowledged.

## References

- 1 M. R. Acocella and G. Guerra, *ChemCatChem*, 2018, **10**, 2350–2359.
- 2 C. Su and K. P. Loh, *Acc. Chem. Res.*, 2013, **46**, 2275–2285.
- 3 M. R. Acocella, A. Vittore, M. Maggio, G. Guerra, L. Giannini and L. Tadiello, *Polymers*, 2019, **11**, 1330.
- 4 M. R. Acocella, M. Maggio, C. Ambrosio, N. Aprea and G. Guerra, *ACS Omega*, 2017, **2**, 7862–7867.
- 5 R. Villano, M. R. Acocella and G. Guerra, *ChemistrySelect*, 2017, **2**, 10559–10564.
- 6 C. Liu, X. Liu, J. Tan, Q. Wang, H. Wen and C. Zhang, *J. Power Sources*, 2017, **342**, 157–164.
- 7 Y. Zhou, L. Liu, Y. Shen, L. Wu, L. Yu, F. Liang and J. Xi, *Chem. Commun.*, 2017, **53**, 7565–7568.
- 8 S. Liang, C. Liang, Y. Xia, H. Xu, H. Huang, X. Tao, Y. Gan and W. Zhang, *J. Power Sources*, 2016, **306**, 200–207.
- 9 S. Zhuang, E. S. Lee, L. Lei, B. B. Nunna, L. Kuang and W. Zhang, *Int. J. Energy Res.*, 2016, **40**, 2136–2149.
- 10 G. Wang, J. Zhang and S. Hou, *Mater. Res. Bull.*, 2016, 454–458.
- 11 C. Schneidermann, N. Jäckel, S. Oswald, L. Giebeler, V. Presser and L. Borchardt, *ChemSusChem*, 2017, **10**, 2416–2424.
- 12 Y. Huang, J. Tang, L. Gai, Y. Gong, H. Guan, R. He and H. Lyu, *Chem. Eng. J.*, 2017, **319**, 229–239.
- 13 S. Xu, M. Wen, J. Li, S. Guo, M. Wang, Q. Du, J. Shen, Y. Zhang and S. Jiang, *Polymer*, 2008, **49**, 4861–4870.
- 14 L. D'Urso, M. Acocella, G. Guerra, V. Iozzino, F. De Santis and R. Pantani, *Polymers*, 2018, **10**, 139.
- 15 L. D'Urso, M. R. Acocella, F. De Santis, G. Guerra and R. Pantani, *Polymer*, 2022, **256**, 125237.
- 16 P. Karami, S. S. Khasraghi, M. Hashemi, S. Rabiei and A. Shojaei, *Adv. Colloid Interface Sci.*, 2019, **269**, 122–151.
- 17 M. H. Islam, S. Afroj, M. A. Uddin, D. V. Andreeva, K. S. Novoselov and N. Karim, *Adv. Funct. Mater.*, 2022, **32**, 2205723.
- 18 Y. Fan, G. D. Fowler and M. Zhao, *J. Cleaner Prod.*, 2020, **247**, 119115.
- 19 L. B. Tunnicliffe and J. J. C. Busfield, in *Designing of Elastomer Nanocomposites: from Theory to Applications*, ed. K. W. Stöckelhuber, A. Das and M. Klüppel, Springer International Publishing, Cham, 2017, pp. 71–102.
- 20 L. Staudenmaier, *Ber. Dtsch. Chem. Ges.*, 1898, **31**, 1481–1487.
- 21 U. Hofmann and E. König, *Z. Anorg. Allg. Chem.*, 1937, **234**, 311–336.
- 22 U. Hofmann and R. Holst, *Ber. Dtsch. Chem. Ges.*, 1939, **72**, 754–771.
- 23 W. S. Hummers and R. E. Offeman, *J. Am. Chem. Soc.*, 1958, **80**, 1339.
- 24 S. Gómez, N. M. Rendtorff, E. F. Aglietti, Y. Sakka and G. Suárez, *Appl. Surf. Sci.*, 2016, **379**, 264–269.
- 25 A. Kiani, M. R. Acocella, V. Granata, E. Mazzotta, C. Malitesta and G. Guerra, *ACS Sustainable Chem. Eng.*, 2022, **10**, 16019–16026.



- 26 J. C. Curtis, R. L. Taylor and G. A. Joyce, Hydrogen peroxide oxidation of Carbon Black, *WO pat.*, 1998032804A1, 1998.
- 27 C. Y. Liu and W. T. Cheng, *Surf. Interface Anal.*, 2019, **51**, 316–325.
- 28 G. Lota, P. Krawczyk, K. Lota, A. Sierczyńska, Ł. Kolanowski, M. Baraniak and T. Buchwald, *J. Solid State Electrochem.*, 2016, **20**, 2857–2864.
- 29 I. Sutherland, E. Sheng, R. H. Bradley and P. K. Freakley, *J. Mater. Sci.*, 1996, **31**, 5651–5655.
- 30 A. Kiani, N. Sozio and M. Rosaria Acocella, *Mol. Syst. Des. Eng.*, 2023, **8**, 942–949.
- 31 H. Wang, Q. Zhao, K. Zhang, F. Wang, J. Zhi and C.-X. Shan, *Langmuir*, 2022, **38**, 11304–11313.
- 32 G. Achagri, Y. Essamlali, O. Amadine, M. Majdoub, A. Chakir and M. Zahouily, *RSC Adv.*, 2020, **10**, 24941–24950.
- 33 One-step nondestructive functionalization of graphene oxide paper with amines - RSC Advances (RSC Publishing), <https://pubs.rsc.org/en/content/articlelanding/2018/ra/c8ra00986d>, accessed 19 March 2024.
- 34 S. Kang, A. R. Jones, J. S. Moore, S. R. White and N. R. Sottos, *Adv. Funct. Mater.*, 2014, **24**, 2947–2956.
- 35 N. Alzate-Carvajal, E. V. Basiuk, V. Meza-Laguna, I. Puente-Lee, M. H. Farías, N. Bogdanchikova and V. A. Basiuk, *RSC Adv.*, 2016, **6**, 113596–113610.
- 36 T.-X. Metro, J. Bonnamour, T. Reidon, J. Sarpoulet, J. Martinez and F. Lamaty, *Chem. Commun.*, 2012, **48**, 11781–11783.
- 37 W. I. Nicholson, F. Barreteau, J. A. Leitch, R. Payne, I. Priestley, E. Godineau, C. Battilocchio and D. L. Browne, *Angew. Chem., Int. Ed.*, 2021, **60**, 21868–21874.
- 38 S. Rani, M. Kumar, R. Kumar, D. Kumar, S. Sharma and G. Singh, *Mater. Res. Bull.*, 2014, **60**, 143–149.
- 39 Y. Matsuo, T. Miyabe, T. Fukutsuka and Y. Sugie, *Carbon*, 2007, **45**, 1005–1012.
- 40 L. R. Knöpke, N. Nemat, A. Köckritz, A. Brückner and U. Bentrup, *ChemCatChem*, 2010, **2**, 273–280.
- 41 D. Luciana, M. R. Acocella, F. De Santis, G. Guerra and R. Pantani, *Polymer*, 2022, **256**, 125237.
- 42 L. R. Snyder, *J. Chromatogr. Sci.*, 1978, **16**, 223–234.
- 43 C. Jimenez-Gonzalez, C. S. Ponder, Q. B. Broxterman and J. B. Manley, *Org. Process Res. Dev.*, 2011, **15**, 912–917.
- 44 K. Van Aken, L. Streckowski and L. Patiny, *Beilstein J. Org. Chem.*, 2006, **2**(3), DOI: [10.1186/1860-5397-2-3](https://doi.org/10.1186/1860-5397-2-3).

